J. Fluid Mech. (2009), *vol.* 634, *pp.* 487–497.
doi:10.1017/S0022112009990711 Printed in the United Kingdom

A prediction for the optimal stratification for turbulent mixing

W. TANG,[1] C. P. CAULFIELD[2,3]† AND R. R. KERSWELL[4]

[1]School of Mathematical & Statistical Sciences, Arizona State University, Tempe, AZ 85287-1804, USA

[2]BP Institute, University of Cambridge, Madingley Road, Cambridge CB3 0EZ, UK

[3]Department of Applied Mathematics and Theoretical Physics, University of Cambridge, Centre for Mathematical Sciences, Wilberforce Road, Cambridge CB3 0WA, UK

[4]School of Mathematics, University of Bristol, University Walk, Bristol BS8 1TW, UK

(Received 21 April 2009 and in revised form 2 June 2009)

By identifying the stratification which leads to maximal buoyancy flux in a stably-stratified plane Couette flow, we make a prediction of what bulk stratification (as a function of the shear) is optimal for turbulent mixing. A previous attempt to do this (Caulfield, Tang & Plasting, *J. Fluid Mech.*, vol. 498, 2004, p. 315) failed due to an unexpected degeneracy in the variational problem. Here, we overcome this issue by parameterizing the variational problem implicitly with the overall mixing efficiency which is then optimized across to return a rigorous upper bound on the buoyancy flux. We find that the bulk Richardson number quickly approaches 1/6 in the asymptotic limit of high shear with the associated mixing efficiency tending to 1/3. The predicted mean profiles associated with the bound appear to have a layered structure, with the gradient Richardson number being low both in the interior, and in boundary layers near the walls, with a global maximum, also equal to 1/6, occurring at the edge of the boundary layers.

1. Introduction

Stratified mixing by small-scale turbulence is a fundamental process in the atmosphere and ocean, which plays a key role in the overall dynamics and global budgets of heat and momentum (Wunsch & Ferrari 2004, Ivey, Winters & Koseff 2008). Parameterizations are needed to embed the effects of small-time and length-scale stratified mixing (typically shear-driven) within larger scale models (Fernando 1991, Peltier & Caulfield 2003). A key concept is the 'mixing efficiency' η, which is the proportion of the work done that leads to irreversible stratified mixing. Conventionally, η is assumed to be at most 0.2 (Osborn 1980) characteristic of numerically simulated Kelvin–Helmholtz billows triggering turbulence (Peltier & Caulfield 2003), although recent experimental evidence from exchange flows (Prastowo *et al.* 2008) suggests that smaller efficiencies may occur in less idealized flows.

It is intuitively appealing, and experimentally verified that η must increase from zero for small values of overall stratification (see Linden 1979; Fernando 1991 for reviews). Linden (1979) further argued that there should typically be an overall stratification

† Email address for correspondence: c.p.caulfield@bpi.cam.ac.uk

where mixing is most efficient. For higher stratifications, mixing is reduced due to diminished vertical motions, although recent research suggests that mixing is never completely suppressed, even when the stratification is very strong, provided the buoyancy Reynolds number $Re_b = \epsilon/(\nu N^2) \gg 1$, where N is the buoyancy frequency, ν is the kinematic viscosity and ϵ is the turbulent dissipation rate (Billant & Chomaz 2001, Brethouwer *et al.* 2007). Such non-monotonic variation of mixing efficiency with overall stratification implies the generic development of 'layers' with regions of relatively well-mixed fluid separated by thin regions of stronger stratification, as originally proposed by Phillips (1972) and Posmentier (1977).

Finding theoretical evidence for a preferred mixing stratification as a function of the shear, and hence the generic development of layers is the motivation for this study. Apart from exhaustive numerical simulations, variational methods arguably provide the only feasible theoretical approach to take given that mixing flows of interest are turbulent. The key idea is to embed all the complication associated with the turbulence into an enlarged set of flow fields which are easier to manipulate and characterize in the sense of bounding quantities of interest. The philosophy pursued here is to look for a flow field which maximizes the mixing at fixed shear but arbitrary stratification subject to a small (to keep things tractable) subset of the dynamical constraints imposed by the governing equations. The optimizing (shear dependent) stratification which emerges is then a theoretically grounded predictor for Linden's observations (Linden 1979). However, finding a non-trivial (< 1) maximum value directly for the mixing efficiency is very difficult and a more natural target for bounding is the closely related buoyancy flux $\mathscr{B}$ which enters into the definition of the mixing efficiency

$$\eta := \frac{\mathscr{B}}{\mathscr{B} + \epsilon}. \tag{1.1}$$

Earlier work (Caulfield & Kerswell 2001; Caulfield, Tang & Plasting 2004) in a stratified plane Couette system isolated a bound on $\mathscr{B}$ which unfortunately failed to yield any information about the optimal stratification field (in the form of the bulk Richardson number J, or indeed the structure of the flow profiles) due to an unexpected degeneracy. The purpose of this paper is to remove this degeneracy to reveal the shear-dependent optimizing stratification for the Caulfield *et al.* (2004) bound. This is achieved by effectively parameterizing the variational problem using an *a priori* unknown variable, the mixing efficiency. In practice, this means adding an extra constraint to those used in Caulfield *et al.* (2004) requiring that the mixing efficiency has the pre-selected value η and then finding a rigorous upper bound $\mathscr{B}^{\eta}_{max}(J, Re; \eta)$. Optimizing over η removes the implicit nature of the bound leaving $\mathscr{B}_{max}(J, Re) = \max_{\eta} \mathscr{B}^{\eta}_{max}(J, Re; \eta)$ which is now a function of the two *a priori* known parameters in the stratified plane Couette problem. A further maximization over J reveals the optimizer $J_{max}(Re)$ and retrieves the bound $\mathscr{B}_{max}(J_{max}(Re), Re) = \max_J \mathscr{B}_{max}(J, Re)$ first derived in Caulfield *et al.* (2004).

The calculations presented here are also interesting from the methodology perspective in two ways. First, while we are successful in our objective (extracting the optimizing stratification), the variational machinery is also found to break down in a way not seen in other applications. For reasons which remain unclear, we are unable to derive a bound on the buoyancy flux for stratifications stronger than the optimal value of J for any Re and η. Second, the approach employed here of deriving a formal inequality result predicated on a 'conditional' constraint is a promising new direction for this variational approach which dates back to initial

ideas of Malkus (1954, 1956) and formulation by Howard (1963) and Busse (1969, 1970). Our conditional constraint builds on previous work by Krommes & Smith (1987) who considered time-dependent conditional constraints for generating bounds on advective transport in turbulent fluids and plasmas, and by Kerswell (2000) who examined the consequences of a 'smoothness' or minimum length scale constraint on an energy dissipation rate bound in shear turbulence.

2. Mathematical formulation

We follow Caulfield *et al.* (2004) by considering stratified plane Couette flow in which a layer of fluid is sheared by two infinite parallel plates at $z=\pm 1/2d$, moving with velocities $\mp 1/2\Delta U\hat{\boldsymbol{x}}$ respectively. There is a constant stable density difference across the layer of $\Delta\rho$, which is sufficiently small to allow the Boussinesq approximation to be invoked. For simplicity, we assume that the Prandtl number (the ratio of the kinematic viscosity to the thermal diffusivity) $\sigma=\nu/\kappa=1$. The plate separation d, a characteristic density ρ_0 (where $\Delta\rho/\rho_0\ll 1$) and the diffusion time scale $d^2/\kappa=d^2/\nu$ (since $\sigma=1$) are used to non-dimensionalize the governing equations:

$$\frac{\partial \boldsymbol{u}}{\partial t}+\boldsymbol{u}\cdot\nabla\boldsymbol{u}+\nabla p-\nabla^2\boldsymbol{u}+Re^2J\rho\,\hat{\mathbf{z}}=\mathbf{0},\ \ \frac{\partial\rho}{\partial t}+\boldsymbol{u}\cdot\nabla\rho-\nabla^2\rho=0,\ \ \nabla\cdot\boldsymbol{u}=0, \quad (2.1a)$$

$$\boldsymbol{u}\left(x,y,\pm\tfrac{1}{2},t\right)=\mp\tfrac{1}{2}Re\hat{\boldsymbol{x}},\ \ \rho\left(x,y,\pm\tfrac{1}{2},t\right)=\mp\tfrac{1}{2},\ \ Re:=\frac{\Delta U d}{\nu},\ \ J:=\frac{g\Delta\rho d}{\rho_0(\Delta U)^2}, \quad (2.1b)$$

where ρ is the (non-dimensional) difference in the density from ρ_0 scaled by $\Delta\rho$, $\boldsymbol{u}=(u_1,u_2,u_3)$, Re is the Reynolds number, J is the (bulk) Richardson number and g is the acceleration due to gravity. We define volume averaging $\langle\ \ \rangle$ and horizontal-and-long-time averaging $\overline{(\ \ )}$ of a quantity q as

$$\langle q(\boldsymbol{x},t)\rangle:=\int_{-1/2}^{1/2}\overline{q}(z)\,\mathrm{d}z:=\int_{-1/2}^{1/2}\left(\lim_{L_x,L_y,T\to\infty}\frac{1}{4L_xL_yT}\int_0^T\int_{-L_x}^{L_x}\int_{-L_y}^{L_y}q(\boldsymbol{x},t)\,\mathrm{d}y\,\mathrm{d}x\,\mathrm{d}t\right)\mathrm{d}z\ . \quad (2.2)$$

Two important quantities characterizing the turbulent motion are the long-time-averaged buoyancy flux $\mathscr{B}$, and the mechanical energy dissipation rate ϵ associated with the mixing in the entire flow

$$\mathscr{B}:=Re^2J\langle\rho u_3\rangle=Re^2J(\langle|\nabla\rho|^2\rangle-1),\qquad \epsilon:=\langle\|\nabla\boldsymbol{u}\|^2\rangle-Re^2, \quad (2.3)$$

where Re^2 is the dissipation rate of the (non-mixing) laminar shear $-Rez\hat{\mathbf{x}}$ realized at low Re. The energy available for mixing, $Re\langle u_1u_3\rangle=\mathscr{B}+\epsilon$, feeds into these two sinks with the mixing efficiency η (defined in (1.1)) indicating the exact split over the entirety of the flow. The (overall) mixing efficiency η is thus a vertical average of the flux Richardson number $Ri_f(z)$, which in this flow is expressed as

$$Ri_f(z)=\frac{Re^2J\overline{\rho u_3}}{Re\overline{u_1u_3}},\ \eta=\langle Ri_f\rangle, \quad (2.4)$$

typically dependent on z (and J and Re) in turbulent stratified shear flows (see, e.g. Armenio & Sarkar 2002).

The approach adopted here is to find the maximum value of the buoyancy flux for a velocity field which only satisfies a small set of dynamical constraints derived directly from the governing equations together with an additional condition that the mixing

efficiency attains a particular value. This is pursued by setting up the Lagrangian functional

$$\begin{aligned}\mathscr{L} := {} & Re^2 J(\langle|\nabla\rho|^2\rangle - 1) + a[Re\langle u_1 u_3\rangle - Re^2 J\langle\rho u_3\rangle - \langle\|\nabla\boldsymbol{u}\|^2\rangle + Re^2] \\ & + ab[1 - \langle|\nabla\rho|^2\rangle + \langle\rho u_3\rangle]Re^2 J - \langle a\phi'(\overline{u_1 u_3} - \bar{u}' - \langle u_1 u_3\rangle - Re)\rangle \\ & - \langle abRe^2 J\tau'(\overline{\rho u_3} - \bar{\rho}' - \langle\rho u_3\rangle - 1)\rangle + \langle a\hat{p}\nabla\cdot\boldsymbol{u}\rangle \\ & - ac[\eta(\|\nabla\boldsymbol{u}\|^2 - Re^2) - (1-\eta)Re^2 J(\langle|\nabla\rho|^2\rangle - 1)],\end{aligned} \tag{2.5}$$

where $(.)' = \mathrm{d}/\mathrm{d}z(.)$. The Lagrange multipliers a, ab, $-a\phi'(z)$, $-abRe^2 J\tau'(z)$ and $a\hat{p}(\boldsymbol{x})$ impose the total kinetic energy balance, entropy flux balance, mean streamwise momentum balance (at fixed z), mean heat balance (at fixed z) and pointwise incompressibility respectively, and $-ac$ imposes the new mixing efficiency condition (a, b and c are scalars). For convenience, the Lagrange multiplier imposing entropy flux balance ab corresponds to the Lagrange multiplier b in Caulfield *et al.* (2004).

To make progress, we use a trick due to Hopf (1941) and developed by Doering & Constantin (1992, 1994, 1996) by adopting a *non-unique* decomposition of the velocity and density fields based upon the Lagrange multiplier fields $\phi(z)$ and $\tau(z)$,

$$\boldsymbol{u}(\boldsymbol{x},t) = \phi(z)\hat{\boldsymbol{x}} + \boldsymbol{v}(\boldsymbol{x},t), \;\; \rho(\boldsymbol{x},t) = \tau(z) + \theta(\boldsymbol{x},t). \tag{2.6}$$

The non-uniqueness stems from the fact that the 'fluctuation' fields $\boldsymbol{v}$ and θ are permitted to have a mean, i.e. $\overline{\boldsymbol{v}} \neq \boldsymbol{0}$ and $\overline{\theta} \neq 0$ in general, yet must satisfy homogeneous boundary conditions, while the 'background' fields $\phi(z)$ and $\tau(z)$ are supposed to satisfy the (inhomogeneous) boundary conditions so that

$$\phi = \mp\tfrac{1}{2}Re, \;\; \tau = \mp\tfrac{1}{2}, \;\; \mathbf{v} = \boldsymbol{0}, \;\; \theta = 0 \text{ at } z = \pm\tfrac{1}{2}. \tag{2.7}$$

Substituting in this decomposition, variations with respect to $\overline{v}_1$ and $\overline{\theta}$ require

$$\overline{v}_1 = -\frac{(1+2c\eta)}{2(1+c\eta)}(\phi + Rez), \quad \overline{\theta} = \frac{(2[1+ac(1-\eta)] - ab))}{2(ab - [1+ac(1-\eta)])}(\tau + z), \tag{2.8}$$

so that the background fields can be related to the mean fields,

$$\overline{u}_1 = \frac{(\phi + Rez)}{2(1+c\eta)} - Rez, \quad \overline{\rho} = \frac{ab(\tau+z)}{2(ab - [1+ac(1-\eta)])} - z. \tag{2.9}$$

With $\hat{\boldsymbol{v}} := \boldsymbol{v} - \overline{v}_1\hat{x}$ and $\hat{\theta} := \theta - \overline{\theta}$ now 'meanless',

$$\mathscr{L} = \frac{a\langle(\phi' + Re)^2\rangle}{4(1+c\eta)} + (ab - [1+ac(1-\eta)])Re^2 J\langle(\overline{\rho}' + 1)^2\rangle - \mathscr{H}, \tag{2.10a}$$

with

$$\begin{aligned}\mathscr{H} := {} & a(1+c\eta)\langle\|\nabla\hat{\boldsymbol{v}}\|^2\rangle + a\langle\hat{\boldsymbol{v}}\cdot\nabla\hat{p}\rangle + a\langle\phi'\hat{v}_1\hat{v}_3\rangle \\ & + Re^2 J([ab - (1+ac[1-\eta])])\langle|\nabla\hat{\theta}|^2\rangle + a\langle\hat{v}_3\hat{\theta}\rangle + ab\langle\tau'\hat{v}_3\hat{\theta}\rangle).\end{aligned} \tag{2.10b}$$

The crux of the analysis is to recognize that if all the Lagrange multipliers can be chosen such that $\mathscr{H} \geqslant 0$ for all incompressible fields $\hat{\boldsymbol{v}}$ and $\hat{\theta}$, then an upper bound exists for $\mathscr{L}$ (Doering & Constantin 1992, 1994, 1996). Minimally, $a > 0$, $c > -1/\eta$ and $ab > 1 + ac(1-\eta)$, otherwise $\mathscr{H}$ can reach $-\infty$ for fields of vanishing length scales. The condition $\mathscr{H} \geqslant 0$ for all allowable $\hat{\boldsymbol{v}}$ and $\hat{\theta}$ amounts to a spectral constraint on a linear operator (Doering & Constantin 1992, 1994, 1996) derived from $\mathscr{H}$ and

parameterized by ϕ and τ. To find the lowest (best) bound on $\mathscr{L}$, all the other Euler–Lagrange equations:

$$\tfrac{1}{2}\lambda(\phi' + Re)(1-\eta) = \overline{\hat{v}_1\hat{v}_3} - \langle \hat{v}_1\hat{v}_3\rangle, \tag{2.11a}$$

$$2\nabla^2\hat{\boldsymbol{v}} - \lambda\phi'(1-\eta)\begin{pmatrix}\hat{v}_3\\0\\\hat{v}_1\end{pmatrix} - (b-1)(1-\eta)\lambda Re^2 J\overline{\rho}'\hat{\theta}\hat{\mathbf{z}} - 1 + c\eta = \mathbf{0}, \tag{2.11b}$$

$$\nabla\cdot\hat{\boldsymbol{v}} = 0,\ \ ab = 2(1+ac[1-\eta]) - a, \quad (b-1)(\nabla^2\hat{\theta} - \overline{\rho}'\hat{v}_3) = 0, \tag{2.11c}$$

$$\overline{\rho}' + 1 + \langle \hat{v}_3\hat{\theta}\rangle - \overline{\hat{v}_3\hat{\theta}} = 0,\ \ \eta Re\langle \hat{v}_1\hat{v}_3\rangle - Re^2 J\langle \hat{v}_3\hat{\theta}\rangle = 0, \tag{2.11d}$$

where

$$\lambda := \frac{1}{(1-\eta)(1+\eta c)} = 2 - \frac{\langle\|\nabla\hat{\boldsymbol{v}}\rangle\|^2\rangle}{(1-\eta)Re\langle\hat{v}_1\hat{v}_3\rangle}\frac{1+(b-1)(1-\eta)Re^2J\langle|\nabla\hat{\theta}|^2\rangle/\langle\|\nabla\hat{\boldsymbol{v}}\|^2\rangle}{1+\frac{1}{2}(b-1)ReJ\langle|\nabla\hat{\theta}|^2\rangle/\langle\hat{v}_1\hat{v}_3\rangle} \tag{2.12}$$

must be solved as well as simultaneously ensuring that the spectral constraint is satisfied.

The numerical solution strategy, as discussed in Plasting & Kerswell (2003) and Caulfield *et al.* (2004), crucially begins from where the laminar state $\mathbf{u} = -Rez\hat{\mathbf{x}}$; $\boldsymbol{v} = \mathbf{0}$; $\rho = -z$; $\theta = 0$, loses energy stability. This occurs when the energy of an arbitrary perturbation $\tilde{\boldsymbol{u}}(\boldsymbol{x},t)$, $\tilde{\rho}(\boldsymbol{x},t)$ of the laminar solution (albeit with zero horizontal mean, homogeneous boundary conditions and mixing efficiency η) is not ensured to decay, or

$$\frac{\mathrm{d}}{\mathrm{d}t}\left\langle\tfrac{1}{2}\tilde{\mathbf{u}}^2\right\rangle = Re\langle\tilde{u}_1\tilde{u}_3\rangle - \frac{1}{(1-\eta)}\langle\|\nabla\tilde{\mathbf{u}}\|^2\rangle > 0. \tag{2.13}$$

The mixing efficiency condition delays the loss of energy stability to $Re = 82.65/(1-\eta)$ compared to the unconstrained result of 82.65 (Joseph 1976) or, from a different perspective, means that there is the constraint $0 \leqslant \eta \leqslant 1 - 82.65/Re$ for mixing to occur.

The spectral constraint ($\mathscr{H} \geqslant 0$ in (2.10*b*)) for the laminar solution ($\phi = -Rez$, $\tau = -z$) requires $a > 0$, and

$$\left[1 + \left(1 - \frac{1}{a}\right)\frac{\eta}{(1-\eta)}\right]\langle\|\nabla\hat{\boldsymbol{v}}\|^2\rangle - Re\langle\hat{v}_1\hat{v}_3\rangle \geqslant 0. \tag{2.14}$$

Marginality of this can be identified with marginality of the energy stability criterion, in the limit where $a\to\infty$, and so $b\to 2c(1-\eta)-1$ using (2.9) and (2.11). The threshold energy stable solution ($\tilde{\mathbf{u}}$, $\tilde{\rho}$) is then the non-trivial solution ($\hat{\boldsymbol{v}}$, $\hat{\theta}$) that marginally satisfies the laminar spectral constraint. This new solution branch is then followed to higher Re until a second fluctuation field becomes marginal with respect to the spectral constraint. At this point, a new solution branch is traced including the contribution of this fluctuation field until a third becomes marginal and so on (see Plasting & Kerswell 2003 for a detailed description).

The degeneracy encountered in Caulfield *et al.* (2004) arose at the initial energy stability bifurcation. For the un-η-coupled problem considered in Caulfield *et al.* (2004), $c = 0$ in the spectral constraint and $\eta = 0$ in the energy stability problem (2.13). The equivalence between these criteria then corresponds to $a = b = 1$. (The simplification (2.14) is not available as the Euler–Lagrange equation for c, the latter in (2.11*d*), is no longer applicable.) This choice leads to a decoupling of the density and velocity fields and the degeneracy experienced in Caulfield *et al.* (2004) – an

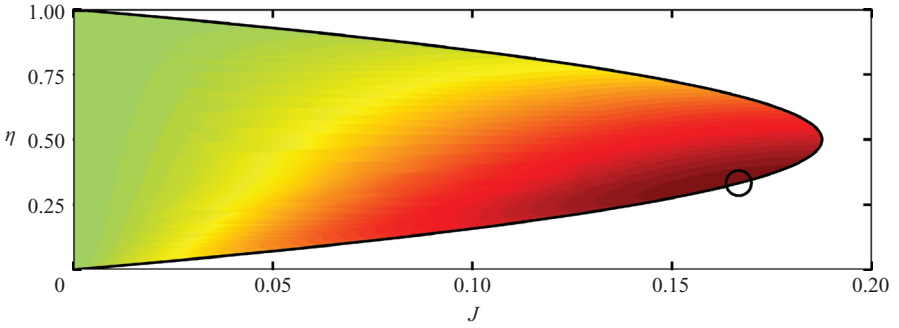

FIGURE 1. Contours of $\mathscr{B}^{\eta}_{max}(J, Re; \eta)/\mathscr{B}_{\infty}$ as J and η is varied for an asymptotically large value $Re = 20000$. The thick solid line marks the envelope of $J^{\eta}_{max}(Re; \eta)$, while the circle marks $J_{max}(Re) \simeq J_{\infty} = 1/6$ which corresponds to $\eta_{max}(Re) \simeq \eta_{\infty} = 1/3$.

indeterminate relationship between $\overline{\rho}'\hat{v}_3$ and $\nabla^2\hat{\theta}$ in the last equation in (2.11c). Crucially with η imposed, this degeneracy only occurs as $b \to 1$, i.e. as J approaches (from below) the value $J^{\eta}_{max}(Re, \eta)$ associated with the maximum buoyancy flux for fixed η and Re. As a result, we are able now to determine the optimizing solution in its entirety by 'unfolding' this limit.

3. Results

In principle, a bound $\mathscr{B}^{\eta}_{max}(J, Re; \eta)$ on the buoyancy flux can be derived over all J, Re and $\eta \leqslant 1 - 82.65/Re$. In practice, we find that the variational machinery breaks down for $J > J^{\eta}_{max}(Re, \eta)$, its optimizing value for given Re and η. This failure manifests itself by the changing of sign of the coefficient $ab-(1+ac[1-\eta])$ of $\langle|\nabla\hat{\theta}|^2\rangle$ in the definition of $\mathscr{H}$. This destroys the possibility of the spectral constraint ever holding and implies that the character of the stationary point sought changes from a global maximum to a saddle. Such a pathology has not been reported before in the literature and quite why it happens here is a mystery. We do know, however, that the result from Caulfield *et al.* (2004) is uniformly valid over J and therefore that the bound $\mathscr{B}^{\eta}_{max}(J_{max}(Re, \eta), Re; \eta)$ holds over $J > J^{\eta}_{max}(Re, \eta)$.

It is straightforward to establish that $\mathscr{B}^{\eta}_{max}(J, Re; \eta)$ increases monotonically with Re, is maximized with respect to variations in η when $c = 0$, and with respect to variations in J when $b = 1$. Figure 1 illustrates the character of our results at a representative large $Re = 20000$. The parabolic line indicates $J = J^{\eta}_{max}(Re, \eta)$ and only for smaller J values (at fixed η) – the coloured region – does the variational analysis yield a bound. (This parabola is actually chopped for $\eta \leqslant 1 - 82.65/Re$, but this is not visible since Re is so large.) Exactly along this line, at $J = J_{max}(Re) := J^{\eta}_{max}(Re, \eta_{max}(Re))$ and $\eta = \eta_{max}(Re)$, the bound is largest (at a given Re) which corresponds to the Caulfield *et al.* (2004) result. Now, crucially, this point is precisely located in the (J, η) plane, and $J_{max}(Re)$ is revealed.

All along this $J = J^{\eta}_{max}(Re, \eta)$ line, there is a connection to the bounding solution outlined in Plasting & Kerswell (2003) for energy dissipation in the unstratified Couette flow problem. The Euler–Lagrange equations (2.12), (2.11a) and (2.11b), combined with the incompressibility condition reduce to (2.13a)–(2.13d) of Plasting & Kerswell (2003), under the transformation

$$Re(1-\eta) = Re_{PK}\,,\ \ \phi(1-\eta) = \phi_{PK}\,,\ \ \lambda(Re) = \lambda_{PK}(Re_{PK})\,, \tag{3.1}$$

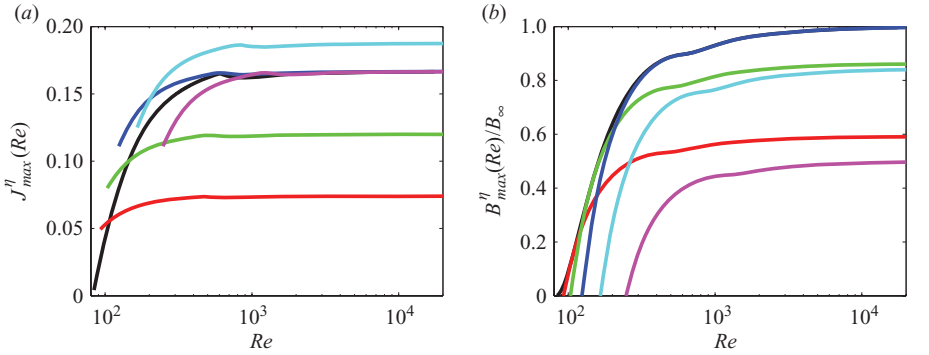

FIGURE 2. (*a*) $J_{max}(Re)$ versus Re (plotted with a black line) $J^{\eta}_{max}(Re, 1/9)$; (red line) $J^{\eta}_{max}(Re, 1/5)$; (green line) $J^{\eta}_{max}(Re, 1/3)$; (blue line) $J^{\eta}_{max}(Re, 1/2)$; (cyan line) $J^{\eta}_{max}(Re, 2/3)$ (magenta line). (*b*) Variation with Re of: $\mathscr{B}_{max}(J_{max}, Re)/\mathscr{B}_{\infty}$; (plotted with a black line), and $\mathscr{B}^{\eta}_{max}(J^{\eta}_{max}, Re; \eta)/\mathscr{B}_{\infty}$ for $\eta = 1/9$; (red line) $\eta = 1/5$; (green line) $\eta = 1/3$; (blue line) $\eta = 1/2$; (cyan line) $\eta = 2/3$; (magenta line). Note that increasing η increases Re at which energy stability is lost.

where the subscript PK refers to the equivalent quantities defined in Plasting & Kerswell (2003) (hereafter, λ_{PK} is understood to be calculated at Re_{PK} for clarity). Therefore, as in the special case of Caulfield *et al.* (2004), the fields ϕ and $\hat{\boldsymbol{v}}$ associated with generating a bound on the long-time averaged buoyancy flux in the more general problem of stratified Couette flow with imposed mixing efficiency can be identified with the fields associated with generating a bound on the dissipation rate in unstratified Couette flow, with appropriate rescaling of Re. Now, however, we can further see that consistency between (2.11*d*) and (2.11*a*), (2.11*c*) and (2.11*b*) requires that the density fields are slaved to the velocity fields,

$$\overline{\rho}'(Re) = \frac{\phi'_{PK}(Re_{PK})}{Re_{PK}}, \quad \hat{\theta}(Re) = \frac{2\hat{v}_1(Re_{PK})}{\lambda_{PK} Re_{PK}}, \quad J^{\eta}_{max}(Re, \eta) = \tfrac{1}{2}\eta(1-\eta)\lambda_{PK}. \tag{3.2}$$

Optimizing over η (equivalent to setting c to 0 in (2.12)) requires

$$\eta_{max}(Re) = \frac{\lambda_{PK} - 1}{\lambda_{PK}} \quad \& \quad J_{max}(Re) = \tfrac{1}{2}\eta_{max}. \tag{3.3}$$

Although the approach of λ_{PK} to its asymptotic value of 3/2 is non-smooth (see figure 2*a*), λ is within 1 % of this value for $Re_{PK} > 1300$. Hence $\eta_{max}(Re) \approx 1/3$ and $J_{max}(Re) \approx 1/3$ for $Re > 1300/(1-\eta) \approx 1950$.

With (3.1), the bound on the buoyancy flux can be constructed straightforwardly from the bound on the dissipation rate calculated in Plasting & Kerswell (2003) as

$$\begin{aligned} \mathscr{B}^{\eta}_{max}\left(J^{\eta}_{max}(Re, \eta), Re; \eta\right) &= \frac{\eta}{(1-\eta)} \frac{\lambda^2_{PK}}{4(\lambda_{PK} - 1)} \langle (\phi'_{PK} + Re_{PK})^2 \rangle, \\ &\to 0.008553 Re^3 \eta (1-\eta)^2 \quad \text{as} \quad Re \to \infty. \end{aligned} \tag{3.4}$$

The asymptotic bound on the buoyancy flux is maximized for $\eta_{\infty} = \lim_{Re\to\infty} \eta_{max}(Re) = 1/3$ which recovers the Caulfield *et al.* (2004) scaling result $\mathscr{B}_{max}(J_{max}(Re), Re) \to 0.0012671 Re^3 = \mathscr{B}_{\infty}$ as $Re \to \infty$, and is suggestive of the numerical results of Riley & de Bruyn Kops (2003). Figure 2(*b*) shows $\mathscr{B}_{max}(J_{max}, Re)/\mathscr{B}_{\infty}$ and $\mathscr{B}^{\eta}_{max}(J^{\eta}_{max}, Re; \eta)/\mathscr{B}_{\infty}$ for various choices of η as functions of Re. $\mathscr{B}_{max}(J_{max}, Re)$ is the envelope of all $\mathscr{B}^{\eta}_{max}(J^{\eta}_{max}, Re; \eta)$ curves for $\eta \leqslant 1/3$ where the point of contact is given by $\eta = \eta_{max}(Re)$ (curves for $\eta > 1/3$ are strictly below the global maximum bound).

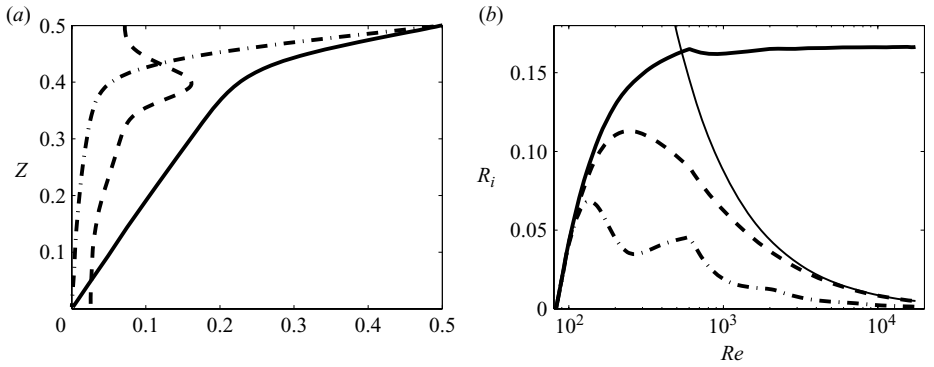

FIGURE 3. (*a*) Variation with z of: $\overline{u}_1$ (plotted with a solid line); $-\overline{\rho}$ (dot-dashed line); and $Ri(z)$ as defined in (3.5) (dashed line) for a flow with $Re = 826.5$ and $J = J_{max}(826.5) = 0.1620$. $Ri(z)$ is even, while $\overline{u}_1$ and $\overline{\rho}$ are odd about the midplane $z = 0$ of the flow. The boundary layer structure is clearly evident, with Ri reaching a maximum $Ri_{max}(Re)$ at the edge of the boundary layer. (*b*) Variation with Re, for flows with $J = J_{max}(Re)$, of: the maximum value $Ri_{max}(Re)$ (i.e. at the edge of the boundary layers, plotted with a solid line); $Ri(1/2, Re)$ (i.e. at the wall, plotted with a dashed line) and $Ri(0, Re)$ (i.e. at the midplane, plotted with a dot-dashed line). The asymptotic scaling for $Ri(1/2, Re)$ identified in Caulfield *et al.* (2004) is plotted with a thin solid line. By comparison with figure 2, $Ri_{max}(Re) = J_{max}(Re)$.

The complete optimal mean flow profiles can also now be deduced. In figure 3(*a*), we plot profiles of $\overline{u}_1$ (solid line) and $-\overline{\rho}$ (dot-dashed line) for a flow with $Re = 826.5 = 10Re_{ES}$ and $J = J_{max}(826.5) = 0.1620$. As discussed in Plasting & Kerswell (2003) and Caulfield *et al.* (2004), the mean velocity profile exhibits a boundary layer structure, and since $\phi \to 0$ as $z \to 0$, $\overline{u}_1 \to -1/2Rez$ in the interior of the flow. Similarly, $\overline{\rho}' \to 0$ for the bounding solution as $z \to 0$ using (3.2), and so the mean density also exhibits a boundary layer structure with a well-mixed interior, as postulated in Caulfield *et al.* (2004).

It is now also possible to calculate the gradient Richardson number $Ri(z)$, the appropriate measure for the relative intensity of the stratification and the shear. Expressed in terms of the non-dimensionalization used here,

$$Ri(z, Re) := -Re^2 J \left(\frac{\mathrm{d}\overline{\rho}}{\mathrm{d}z}\right) \Bigg/ \left(\frac{\mathrm{d}\overline{u}_1}{\mathrm{d}z}\right)^2 = \frac{-4J_{max}(Re)Re_{PK}\phi'_{PK}}{(\phi'_{PK} - Re_{PK})^2}, \tag{3.5}$$

for the bounding flow at $\eta_{max}(Re)$ and $J_{max}(Re; \eta_{max})$ using (3.2) and (2.9) and is plotted with a dashed line in figure 3(*a*). As discussed in detail in Caulfield *et al.* (2004), even though the density gradient is large near the wall, since $\phi'_{PK} = O(Re_{PK}^{3/2})$, $Ri(1/2, Re) \to Re^2/(9\mathscr{B}_\infty) \simeq 87.69/Re$ as $Re \to \infty$. In figure 3(*b*), we plot $Ri(1/2, Re)$ with a dashed line, and this asymptotic prediction from Caulfield *et al.* (2004) with a thin solid line. Similarly, since $\phi' \to 0$ as $Re \to \infty$, the interior of the flow becomes well mixed, with $Ri(0, Re)$ tending rapidly to very small values as $Re \to \infty$, as shown in figure 3(*b*) with a dot-dashed line.

Simple analysis of (3.5) shows that the maximum value of $Ri(z, Re)$ over z, $Ri_{max}(Re) = J_{max}(Re)$, where $\phi'_{PK}(z) = Re_{PK}$, which occurs at the edge of the boundary layer. The variation of $Ri_{max}(Re)$ with Re is plotted on figure 3(*b*) with a solid line which is identical to the solid black line ($J_{max}(Re)$) in figure 2(*a*). Therefore, as Re increases, the Richardson number in the interior of the flow (and at the boundaries)

drops towards zero, while for the bounding solution the maximum value of Ri is identical to the value of the bulk Richardson number $J_{max}(Re)$, and is located at some distance from the boundaries. This is highly suggestive that the optimal flow for mixing leads inevitably in its interior to layering as discussed by Linden (1979).

4. Summary

In this paper, an upper limit on the long-time-averaged buoyancy flux within stably stratified plane Couette flow has been derived using a small subset of kinematic and dynamical constraints deduced directly from the governing Navier–Stokes equations. Using a novel trick of further constraining the problem to have a particular mixing efficiency, we have uncovered the optimal bulk Richardson number $J_{max}(Re)$ (and hence bulk stratification) associated with this maximum as a function of the shear. The asymptotic value of $J_{max}(Re) \to 1/6$ is consistent with the picture put forward by Linden (1979) that there is an optimal stratification most conducive to mixing, that this stratification inevitably leads to a layered flow structure, and that at high Re, mixing efficiency is finite implying that the dissipation and buoyancy flux have the same scaling. This generic development of layers suggests that caution needs to be shown in applying concepts from idealized flow models with uniform density gradients, while an interesting question arises as to how to identify the characteristic depth of such layers in open flows.

The buoyancy flux bound presented in this paper has been derived as a general function of the stratification and shear, both *a priori* known parameters of the stratified plane Couette flow problem. This two-parameter result is eminently testable by direct numerical simulations with the key concerns being whether the *qualitative* features of the bound mirror the real behaviour (maxima) of the buoyancy flux and the subsequent relationship with the mixing efficiency. Hopefully this report will stimulate such simulations which may also reveal additional constraints to incorporate into the analysis, will show whether the development of layers is indeed generic, and also will reveal how significant the boundary layers are to the mixing dynamics. Interestingly, the boundary layers associated with these bounding flows are very reminiscent of those observed in numerical simulations of other stratified boundary layers. Both Saiki, Moeng & Sullivan (2000) and Armenio & Sarkar (2002) (who numerically simulated the stable atmospheric boundary layer and channel flow with constant temperature walls, respectively) observed naturally developing boundary layers with low local $Ri(z)$ analogous to the profiles shown in figure 3(a) near $z = 0.5$, even though the flows have markedly different outer conditions.

Certainly, further constraints derived directly from the governing equations can only improve the quality of the output bound. In practice, however, this has proved extremely hard to implement. For example, the original set of constraints used by Busse (1970) to bound the energy dissipation rate in unstratified plane Couette flow (and which form the core of what are used here) has been exhausted only relatively recently (Plasting & Kerswell 2003). Tellingly, Busse's nearly 40-year-old asymptotic result is still essentially unbettered (Kerswell & Soward 1996). It may well be that to improve the optimal stratification prediction made here, rigour needs to be abandoned in favour of pragmatism with new constraints imposed based upon observed features suggested by simulation and experiment, perhaps associated with layer-like characteristics of the horizontally averaged flow or vertical variation of the flux Richardson number $Ri_f(z)$ as defined in (2.4). Such constraints would perhaps

allow the dynamics of the flow's interior to be isolated from the boundaries, thus leading to results more broadly applicable to open flows.

C. P. Caulfield and W. Tang would like to thank the National Science Foundation for support under the Collaborations in Mathematical Geosciences (CMG) initiative (ATM-0222104). C. P. Caulfield would also like to acknowledge the support of the EU Marie Curie International Reintegration Grant MIRG-CT-2005-016563. We also gratefully acknowledge the hospitality of the 2008 GFD Program at Woods Hole Oceanographic Institution and the 'Nature of High Reynolds Turbulence' programme at the Isaac Newton Institute for Mathematical Sciences.

REFERENCES

Armenio, V. & Sarkar, S. 2002 An investigation of stably stratified turbulent channel flow using large-eddy simulation. *J. Fluid Mech.* **459**, 1–42.

Billant, P. & Chomaz, J.-M. 2001 Self-similarity of strongly stratified inviscid flows. *Phys. Fluids* **13**, 1645–1651.

Brethouwer, G., Billant, P., Lindborg, E. & Chomaz, J.-M. 2007 Scaling analysis and simulation of strongly stratified turbulent flows. *J. Fluid Mech.* **585**, 343–368.

Busse, F. H. 1969 On Howard's upper bound for heat transport by turbulent convection. *J. Fluid Mech.* **37**, 457–477.

Busse, F. H. 1970 Bounds for turbulent shear flow. *J. Fluid Mech.* **41**, 219–240.

Caulfield, C. P. & Kerswell, R. R. 2001 Maximal mixing rate in turbulent stably stratified Couette flow. *Phys. Fluids* **13**, 894–900.

Caulfield, C. P., Tang, W. & Plasting, S. C. 2004 Reynolds number dependence of an upper bound for the long-time-averaged buoyancy flux in a plane stratified Couette flow. *J. Fluid Mech.* **498**, 315–332.

Doering, C. R. & Constantin, P. 1992 Energy dissipation in shear driven turbulence. *Phys. Rev. Lett.* **69**, 1648–1651.

Doering, C. R. & Constantin, P. 1994 Variational bounds on energy dissipation in incompressible flows: shear flow. *Phys. Rev.* E **49**, 4087–4099.

Doering, C. R. & Constantin, P. 1996 Variational bounds on energy dissipation in incompressible flows. III. Convection. *Phys. Rev.* E **53**, 5957–5981.

Fernando, H. J. S. 1991 Turbulent mixing in stratified fluids. *Annu. Rev. Fluid Mech.* **23**, 455–493.

Hopf, E. 1941 Ein allgemeiner endlichkeitssatz der hydrodynamik. *Math. Ann.* **117**, 764–775.

Howard, L. N. 1963 Heat transport by turbulent convection. *J. Fluid Mech.* **17**, 405–432.

Ivey, G. N., Winters, K. B. & Koseff J. R. 2008 Density stratification, turbulence, but how much mixing? *Annu. Rev. Fluid Mech.* **40**, 169–184.

Joseph, D. D. 1976 *Stability of Fluid Motions I*. Springer.

Kerswell, R. R. 2000 Lowering dissipation bounds for turbulent flows using a smoothness constraint. *Phys. Lett.* A **272**, 230–235.

Kerswell, R. R. & Soward, A. M. 1996 Upper bounds for turbulent Couette flow incorporating the poloidal power constraint. *J. Fluid Mech.* **328**, 161–176.

Krommes, J. A. & Smith, R. A. 1987 Rigorous upper bounds for transport due to passive advection by inhomogeneous turbulence. *Ann. Phys.* **177**, 246–329.

Linden, P. F. 1979 Mixing in stratified fluids. *Geophys. Astrophys. Fluid Dyn.* **13**, 2–23.

Malkus, W. V. R. 1954 The heat transport and spectrum of thermal turbulence. *Proc. R. Soc.* **225**, 196–212.

Malkus, W. V. R. 1956 Outline of a theory for turbulent shear flow. *J. Fluid Mech.* **1**, 521–539.

Osborn, T. R. 1980 Estimates of the local-rate of vertical diffusion from dissipation measurements. *J. Phys. Oceanogr.* **10**, 83–89.

Peltier, W. R. & Caulfield C. P. 2003 Mixing efficiency in stratified shear flows. *Annu. Rev. Fluid Mech.* **35**, 135–167.

Phillips, O. M. 1972 Turbulence in a strongly stratified fluid is unstable? *Deep Sea Res.* **19**, 79–81.

Plasting, S. C. & Kerswell, R. R. 2003 Improved upper bound on the energy dissipation rate in plane Couette flow: the full solution to Busse's problem and the Constantin–Doering–Hopf problem with one-dimensional background field. *J. Fluid Mech.* **477**, 363–379.

Posmentier, E. S. 1977 The generation of salinity fine structures by vertical diffusion. *J. Phys. Oceanogr.* **7**, 298–300.

Prastowo, T., Griffiths, R. W., Hughes, G. O. & Hogg, A. M. 2008 Mixing efficiency in controlled exchange flows. *J. Fluid Mech.* **600**, 235–244.

Riley, J. J. & de Bruyn Kops, S. M. 2003 Dynamics of turbulence strongly influenced by buoyancy. *Phys. Fluids* **15**, 2047–2059.

Saiki, E. M., Moeng, C.-H. & Sullivan, P. P. 2000 Large-eddy simulation of the stably stratified planetary boundary layer. *Bound.-layer Meteorol.* **95**, 1–30.

Wunsch C. & Ferrari, R. 2004 Vertical mixing, energy and the general circulation of the oceans. *Annu. Rev. Fluid Mech.* **36**, 281–314.